

# Influence of RF power on the properties of sputtered ZnO:Al thin films

Aldrin Antony\*, Paz Carreras, Thomas Keitzl, Rubén Roldán, Oriol Nos, Paolo Frigeri, José Miguel Asensi, and Joan Bertomeu

Grup d'Energia Solar, Universitat de Barcelona, Martí i Franquès 1–11, 08028 Barcelona, Spain

\* Correspondence to: A.A. (aldrianantony@ub.edu)

Transparent conducting, aluminium doped zinc oxide thin films (ZnO:Al) were deposited by radio frequency (RF) magnetron sputtering. The RF power was varied from 60 to 350 W whereas the substrate temperature was kept at 160 °C. The structural, electrical and optical properties of the as-deposited films were found to be influenced by the deposition power. The X-ray diffraction analysis showed that all the films have a strong preferred orientation along the [001] direction. The crystallite size was varied from 14 to 36 nm, however no significant change was observed in the case of lattice constant. The optical band gap varied in the range 3.44–3.58 eV. The lowest resistivity of  $1.2 \times 10^{-3} \Omega \text{ cm}$  was shown by the films deposited at 250 W. The mobility of the films was found to increase with the deposition power.

## 1 Introduction

Transparent conducting oxides (TCO) have a wide range of applications due to their high transparency in the visible region and high conductivity. They are widely used in optoelectronics as well as in many fields like architecture, medicine or cosmetics [1–3]. Recently TCO based on zinc oxide have gained much attention due to their non toxicity, bio compatibility, material abundance and low cost. ZnO offers several advantages like capability to be processed at room or low temperatures, high electron mobility and shows a strong resistance to high energy radiation. ZnO is thermally and chemically stable and is lithography compatible [4]. Undoped ZnO has been used as UV and ozone sensors [5] and also as the active layer in transparent thin film transistors [4, 6]. Impurity (B-, Al-, Ga-, In-) doped ZnO is an n-type degenerate semiconductor with similar electrical and optical properties to ITO [7]. Recently Ga doped ZnO are receiving special attention and has been successfully used to fabricate fully transparent TFTs and as the front TCO for silicon thin film solar cells [4, 8]. Aluminium doped Zinc Oxide (ZnO:Al) has become an integral part of the thin film Si solar cells, as the TCO front contact and also as the back reflector component and contributes to the current gain by light scattering

improvement [9–13].

ZnO:Al thin films can be prepared by a variety of techniques, such as low pressure chemical vapour deposition, sol-gel, chemical spray, pulsed laser deposition, DC and radio frequency (RF) magnetron sputtering, etc. Among the different techniques RF magnetron sputtering is the widely used one which is quite simple and can be applied on large area. The films deposited by this technique exhibit good adhesion to the substrate and a high packing density [7, 11]. In this work ZnO:Al thin films have been deposited by RF magnetron sputtering. The films were deposited at various powers ranging from 60 to 350 W, and the influence of RF power on the electrical, optical and structural properties of ZnO:Al thin films was systematically investigated.

## 2 Experimental

ZnO:Al thin films were deposited onto  $10 \times 10 \text{ cm}^2$  Corning glass (1737F) substrates by RF magnetron sputtering of ZnO:Al target (3 in. diameter) containing 98 wt% ZnO and 2 wt% of  $\text{Al}_2\text{O}_3$  of 99.9% purity. The base pressure in the chamber was always below  $2 \times 10^{-6}$  Torr. The sputtering was carried out in argon atmosphere at a pressure of 3 mTorr. The target

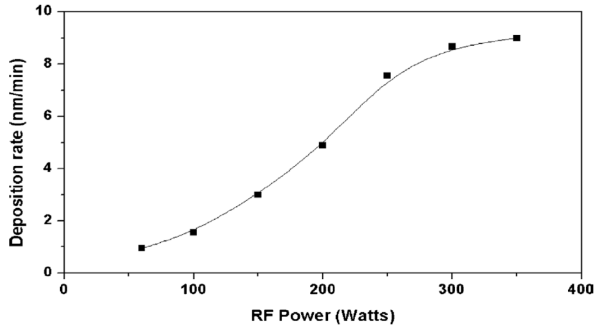


**Figure 1:** The deposition rate of ZnO:Al thin films deposited at different RF powers (line is added to guide the eye).

to substrate distance was fixed at 15 cm to achieve better homogeneity. The films were deposited at a substrate temperature of 160 °C and the RF power was varied in the range 60–350 W. All depositions were done for a constant deposition time of 45 min. The deposition rate was found to increase proportional to the power till 250 W and then reached saturation as shown in Fig. 1. The layers deposited had a good adhesion, physical stability as well as good homogeneity.

The film thickness was measured by using a Dektak 3030 profilometer. The crystallinity of the films was analysed using a powder X-ray diffractometer (PANalytical X’Pert PRO MPD Alpha1 powder system), using copper  $K_{\alpha}$  radiation ( $\lambda = 1.5406 \text{ \AA}$ ) as a source. Transmission and reflection spectra of the samples were recorded by using a UV–Vis–NIR spectrophotometer (Perkin Elmer Lambda 19) with air as the reference. The sheet resistance was measured by using a Jandel RM3 four point probe system. Mobility ( $\mu$ ) and carrier concentration ( $n$ ) were determined from the Hall effect measurements by using standard Van der Pauw method in a magnetic field of 0.3 T.

### 3 Results and discussion

The as deposited films were physically stable and showed a good adherence to the substrate. No cracks or peel-off of the films was observed. X-ray diffraction (XRD) pattern of the ZnO:Al films grown by RF magnetron sputtering at various RF powers is shown in Fig. 2. All the samples showed a diffraction peak at around  $2\theta = 34.4^{\circ}$  and an additional second peak of lower intensity at  $72.48^{\circ}$ .

The first peak at  $34.48^{\circ}$  corresponds to the (002) plane and the second one at  $72.48^{\circ}$  to the second diffraction order (004). This implies a hexagonal wurtzite structure having a strong preferred orientation along the [001] direction with the c-axis perpendicular to the substrate surface. No  $\text{Al}_2\text{O}_3$  re-

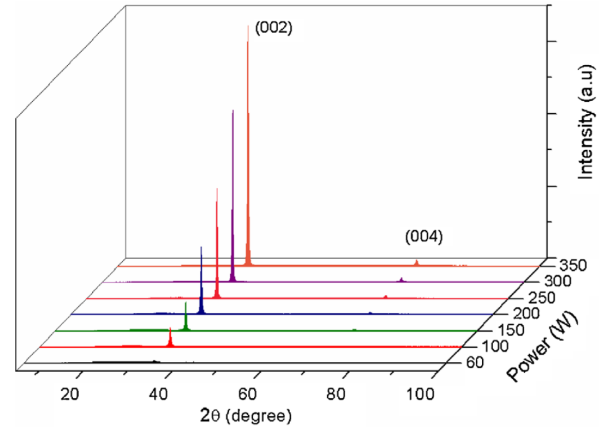


**Figure 2:** (online colour at: [www.pss-a.com](http://www.pss-a.com)) XRD patterns of ZnO:Al thin films deposited at different RF powers.

lated phases could be detected in the XRD patterns. It suggests that aluminium substitutionally replaces zinc in the hexagonal lattice or Al segregates to the non-crystalline region in grain boundary [14].

The full-width at half maximum (FWHM), the integral breadth ( $b$ ) and the Gaussian and Lorentzian part of the integral breadth ( $\beta_G$ ,  $\beta_L$ ) were deduced from the pseudo-Voigt peak profile fitting of the XRD pattern [15]. The instrumental broadening correction has been applied to calculate the integral breadth. The average size of the crystallites ( $\langle D \rangle$ ) was calculated by using the integral breadth as shown in Eq. (1):

$$\langle D \rangle = \lambda / \beta \cos \theta, \quad (1)$$

where  $\beta$  is the integral breadth,  $\lambda$  the X-ray wavelength, and  $\theta$  is the Bragg’s angle of diffraction corresponding to the diffraction peak.

The film microstrain ( $\langle \epsilon \rangle$ ) in the diffracting volume was calculated using the Eq. (2):

$$\langle \epsilon \rangle = \beta_G / 4 \tan \theta, \quad (2)$$

where  $\beta_G$  is the Gaussian part of the integral breadth.

The average crystallite size as a function of the RF power is shown in Fig. 3. The crystallite size increased with power and presented a highest value of 36 nm at 250 W. However, further increase in RF power resulted in slight decrease of crystallite size. The lowest microstrain was obtained for the film deposited at 250 W. The lattice parameter value  $c$ , and the microstrain of the films are shown in Fig. 4. The lattice parameter  $c$  was found to be consistent with the standard value (0.521 nm) and no appreciable change in  $c$  value was observed with the further change in RF power.

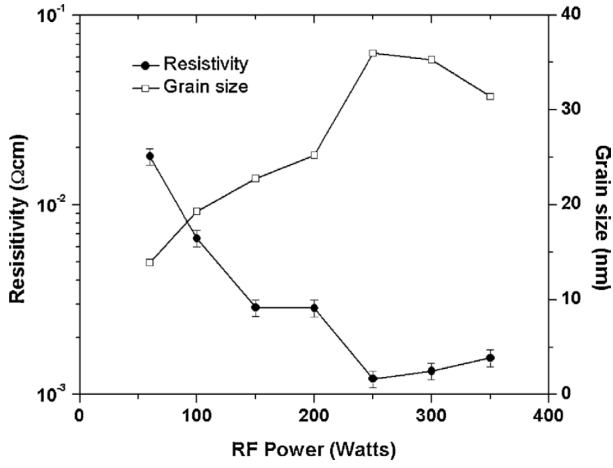


**Figure 3:** The variation of grain size and electrical resistivity of the ZnO:Al thin films deposited at different RF powers (all lines are added to guide the eye).

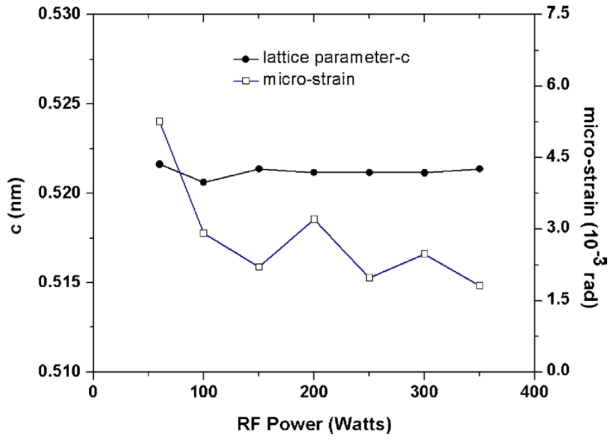


**Figure 4:** (online colour at: [www.pss-a.com](http://www.pss-a.com)) The variation of lattice parameter and micro-strain of the ZnO:Al thin films deposited at different RF powers (all lines are added to guide the eye).

The transmission spectra of the ZnO:Al films grown at various RF powers are shown in Fig. 5. All the films were highly transparent in the visible region of the electromagnetic spectrum. The average transmission in the visible region was more than 80%. The near-infrared transmittance of the films decreased with the increase in RF power. The thickness of the films was found to increase with the increase in RF power, and the main cause for this reduction in transmission was due to the increase in thickness of the films [8]. The decrease in transmission in the near-infrared is also due to the free carrier absorption, which increases with the increase in carrier concentration. The deposition at higher RF powers produces oxygen vacancies in the film resulting in the increase

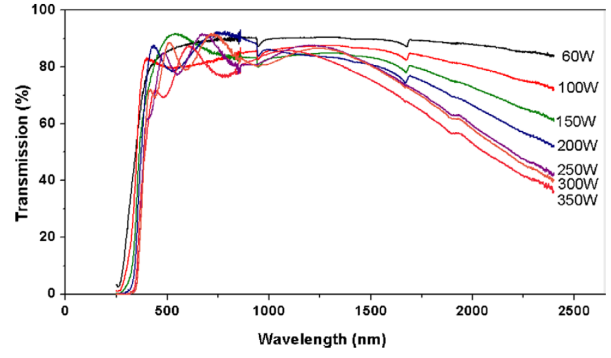


**Figure 5:** (online colour at: [www.pss-a.com](http://www.pss-a.com)) The transmission curves of ZnO:Al thin films deposited at different RF powers.

of free carrier absorption [16].

The absorption coefficient ( $\alpha$ ) was determined from the transmittance and reflectance value by means of Eq. (3) [17].

$$T = (1 - R)^2 e^{-\alpha d}, \quad (3)$$

where  $d$  is the layer thickness,  $R$  the reflectance and  $T$  is the transmittance.

For direct transitions, as in case of ZnO:Al films, the absorption coefficient is given by Eq. (4) [17].

$$\alpha(h\nu) = A^*(h\nu - E_g)^{1/2}, \quad (4)$$

where  $h\nu$  is the incident photon energy,  $E_g$  is the bandgap energy and  $A^*$  is a constant.

The band gap of ZnO:Al films was determined from the plot of  $(\alpha h\nu)^2$  against  $h\nu$  by extrapolating the linear portion of the curve to  $(\alpha h\nu)^2$  equals zero. The calculated values of band gap energies of the ZnO:Al films deposited at various RF powers are shown in Fig. 6. The inset of Fig. 6 shows a typical  $(\alpha h\nu)^2$  against  $(h\nu)$  plot of ZnO:Al thin film deposited at 150 W. The band gap values showed an increase with RF power and attained the highest value of 3.58 eV at 150 W. Beyond 200 W, the band gap value again decreased.

The resistivity of the as-deposited ZnO:Al films decreased as power increased till 250 W, where it showed the lowest value ( $1.2 \times 10^{-3} \Omega \text{ cm}$ ). No significant change in resistivity was observed for higher powers. Figure 3 shows the measured resistivity values of the ZnO:Al films deposited at different powers. The conductivity of ZnO:Al thin films resulted from the ability of the ZnO lattice to incorporate substitutional Al atoms without major structural modification as well as from the scattering mechanisms of the free electrons. When  $\text{Zn}^{2+}$  is replaced by  $\text{Al}^{3+}$ , one free electron is created. Doubly charged oxygen vacancy creates two free electrons. The increase in

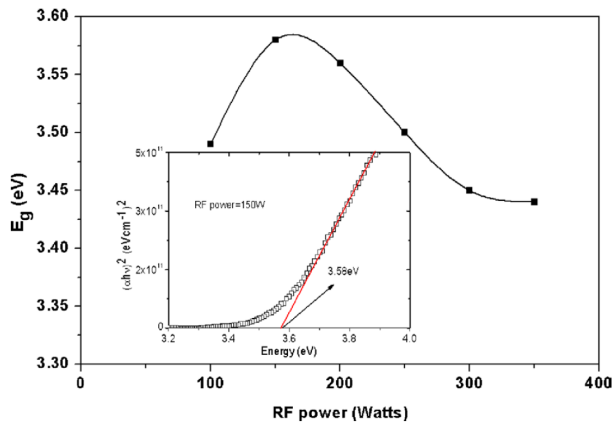


**Figure 6:** (online colour at: [www.pss-a.com](http://www.pss-a.com)) Band gap energies of the ZnO:Al films deposited at various RF powers. The inset shows a typical  $(\alpha h\nu)^2$  against  $(h\nu)$  plot of ZnO:Al thin film deposited at 150 W (line is added to guide the eye).

number of free carriers with increase in RF power reduces the resistivity of the films. The increase in mobility and crystallinity of the films are also responsible for the decrease in resistivity with increase in power [18]. The values of carrier concentration and mobility of the films with RF power are shown in Fig. 7. The carrier concentration increased with the sputtering power and reached a maximum value of  $1.9 \times 10^{20} \text{ cm}^{-3}$  at 150 W and then decreased with increase in power. Mobility was low at lower sputtering powers, but showed a rapid increase beyond 200 W. A highest mobility of  $19 \text{ cm}^2 \text{ V}^{-1} \text{ s}^{-1}$  was observed for the films deposited at 350 W power.

In the low power region, the decrease in resistivity can be ascribed to the increase in free carriers created by the substitutional doping. The small crystallite size in this low power region suggests that the low values of mobility might be due to the scattering at the grain boundaries. The thickness of the films was low for the lower powers of deposition. The thinner films contain more defects than thicker films and increased scattering of carriers takes place resulting in low mobility [4]. In the higher power region, the XRD analysis showed that the crystallinity improved with RF power, and crystallite size showed a maximum value at 250 W. Bigger crystallites weakened the intercrystallite boundary scattering and increased the carrier life time [8]. Consequently an increase in mobility was observed for the films grown at higher powers. In addition, desorption of oxygen from the film at higher deposition powers may also contribute to this low resistivity.

The variation in band gap with RF power can be explained considering the carrier concentration. The band gap increased with the increase in carrier con-

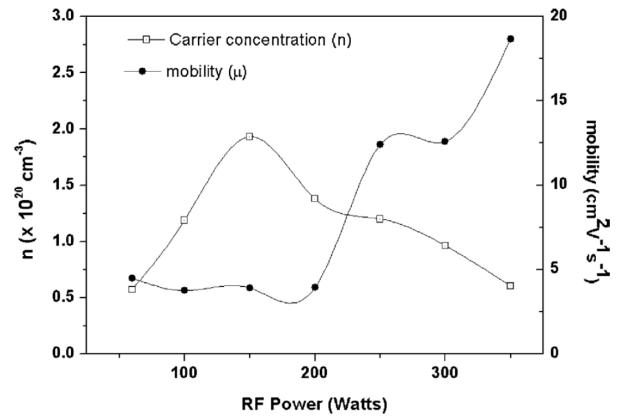


**Figure 7:** The variation of carrier concentration and mobility of the ZnO:Al thin films deposited at different RF powers (all lines are added to guide the eye).

centration. The highest carrier concentration was measured at the deposition power of 150 W, and the energy band gap also showed a maximum value of 3.58 eV at this power. This behaviour of band gap broadening with the increase in carrier concentration is due to Burstein–Moss effect. As the amount of free carriers increases, the Fermi level moves to higher values because the energy required to activate an electron from the valence band to the conduction band is more than the fundamental band gap.

## 4 Conclusion

The RF deposition power was found to influence the structural, electrical and optical properties of ZnO:Al thin films. The increase in RF deposition power increased the plasma energy and produced compact and dense films. The ZnO:Al films deposited at 250 W and above showed lowest resistivity and a highest mobility of  $19 \text{ cm}^2 \text{ V}^{-1} \text{ s}^{-1}$  was obtained for the films deposited at 350 W. All the as deposited films showed transmittance  $>80\%$  in the visible wavelength of light. The results can be useful for the deposition of ZnO:Al thin films onto plastic substrates since a compatible substrate temperature of  $160 \text{ }^\circ\text{C}$  was used in this study. Further work is under way to fabricate thin film solar cells on ZnO:Al coated PEN substrates.

## Acknowledgments

This work has been supported by the Ministerio de Ciencia e Innovación through the projects CLASICO (ENE2007-67742-C04-03) and MICROSIL08 (PSE-120000-2008-1).

This is the accepted version of the following article: Antony, A., Carreras, P., Keitzl, T., Roldán, R., Nos, O., Frigeri, P., Miguel Asensi, J. and Bertomeu, J. (2010), *Influence of RF power on the properties of sputtered ZnO:Al thin films*. Phys. Status Solidi A, 207: 1577–1580., which has been published in final form at [doi:10.1002/pssa.200983765](https://doi.org/10.1002/pssa.200983765).

## References

- [1] C. Klingshirn. *ZnO: From basics towards applications*. Physica Status Solidi B-Basic Solid State Physics **244**, 3027–3073 (September 2007).
- [2] B. G. Lewis and D. C. Paine. *Applications and processing of transparent conducting oxides*. Mrs Bulletin **25**, 22–27 (August 2000).
- [3] E. Fortunato, D. Ginley, H. Hosono, and D. C. Paine. *Transparent conducting oxides for photovoltaics*. Mrs Bulletin **32**, 242–247 (March 2007).
- [4] E. Fortunato, L. Raniero, L. Silva, A. Goncalves, A. Pimentel, P. Barquinha, H. Aguas, L. Pereira, G. Goncalves, I. Ferreira, E. Elangovan, and R. Martins. *Highly stable transparent and conducting gallium-doped zinc oxide thin films for photovoltaic applications*. Solar Energy Materials and Solar Cells **92**, 1605–1610 (December 2008).
- [5] R. Martins, E. Fortunato, P. Nunes, I. Ferreira, A. Marques, M. Bender, N. Katsarakis, V. Cimalla, and G. Kiriakidis. *Zinc oxide as an ozone sensor*. Journal of Applied Physics **96**, 1398–1408 (August 2004).
- [6] E. M. C. Fortunato, P. M. C. Barquinha, A. Pimentel, A. M. F. Goncalves, A. J. S. Marques, L. M. N. Pereira, and R. F. P. Martins. *Fully transparent ZnO thin-film transistor produced at room temperature*. Advanced Materials **17**, 590 (March 2005).
- [7] W. Yang, Z. Liu, D.-L. Peng, F. Zhang, H. Huang, Y. Xie, and Z. Wu. *Room-temperature deposition of transparent conducting Al-doped ZnO films by RF magnetron sputtering method*. Applied Surface Science **255**, 5669–5673 (March 2009).
- [8] E. Fortunato, A. Goncalves, A. Pimentel, P. Barquinha, G. Goncalves, L. Pereira, I. Ferreira, and R. Martins. *Zinc oxide, a multifunctional material: from material to device applications*. Applied Physics a-Materials Science & Processing **96**, 197–205 (July 2009).
- [9] W. Beyer, J. Huepkes, and H. Stiebig. *Transparent conducting oxide films for thin film silicon photovoltaics*. Thin Solid Films **516**, 147–154 (December 2007).
- [10] F. Villar, A. Antony, J. Escarre, D. Ibarz, R. Roldan, M. Stella, D. Munoz, J. M. Asensi, and J. Bertomeu. *Amorphous silicon thin film solar cells deposited entirely by hot-wire chemical vapour deposition at low temperature (< 150 degrees C)*. Thin Solid Films **517**, 3575–3577 (April 2009).
- [11] A. M. K. Dagamseh, B. Vet, F. D. Tichelaar, P. Sutta, and M. Zeman. *ZnO : Al films prepared by rf magnetron sputtering applied as back reflectors in thin-film silicon solar cells*. Thin Solid Films **516**, 7844–7850 (September 2008).
- [12] A. Shah, P. Torres, R. Tscharnner, N. Wyrsh, and H. Keppner. *Photovoltaic technology: The case for thin-film solar cells*. Science **285**, 692–698 (July 1999).
- [13] S. Fay, L. Feitknecht, R. Schluchter, U. Kroll, E. Vallat-Sauvain, and A. Shah. *Rough ZnO layers by LP-CVD process and their effect in improving performances of amorphous and microcrystalline silicon solar cells*. Solar Energy Materials and Solar Cells **90**, 2960–2967 (November 2006).
- [14] J.-H. Lee and J.-T. Song. *Dependence of the electrical and optical properties on the bias voltage for ZnO : Al films deposited by r.f. magnetron sputtering*. Thin Solid Films **516**, 1377–1381 (February 2008).
- [15] R. Delhez, T. Dekeijser, and E. Mittemeijer. *Determination of Crystallite Size and Lattice-Distortions Through X-Ray-Diffraction Line-Profile Analysis - Recipes, Methods and Comments*. Fresenius Zeitschrift Fur Analytische Chemie **312**, 1–16 (1982).
- [16] M. Nisha and M. K. Jayaraj. *Influence of RF power and fluorine doping on the properties of sputtered ITO thin films*. Applied Surface Science **255**, 1790–1795 (December 2008).
- [17] J. Pankove. *Optical properties in semiconductors*. Dove Publication Inc., New York (1971).
- [18] H. Kim, J. S. Horwitz, W. H. Kim, Z. H. Kafafi, and D. B. Chrisey. *Highly oriented indium tin oxide films for high efficiency organic light-emitting diodes*. Journal of Applied Physics **91**, 5371–5376 (April 2002).